SAND2012-5458C

Application of the Conformal Decomposition Finite Element Method to Problems with Capillary Free Surfaces

for

Rekha Rao, David Noble, Christopher Brotherton, Scott Roberts, Christine Roberts, Martin Nemer

10th World Congress on Computational Mechanics

Sao Paulo, Brazil

July 8-13, 2012

LDRD
LABORATORY DIRECTED RESEARCH & DEVELOPMENT

Sandia National Laboratories

Finite Element Methods for Interfaces in Fluid/Thermal Applications

- **Boundary Fitted Meshes**
  - Supports wide variety of interfacial conditions accurately
  - Requires boundary fitted mesh generation
  - Not feasible for arbitrary topological evolution (ALE)
    - Mesh quality degrades with evolution, phase breakup and merging are precluded.
- **eXtended Finite Element Methods (XFEM)**
  - Dolbow et al. (2000), Belytchko et al. (2001)
  - Successfully applied to numerous problems ranging from crack propagation to phase change to multiphase flow
  - Supports weak conditions accurately, mixed and Dirichlet conditions are actively researched (Dolbow et al.)
  - Avoids boundary fitted mesh generation
  - Supports general topological evolution (subject to resolution requirements)
- **Generalized Finite Element Methods (GFEM)**
  - Strouboulis et al. (2000)
  - Combination of standard finite element and partition of unity enrichment
- **Immersed Finite Element Methods**
  - Li et al. (2003), Ilinca and Hetu (2010)
  - Supports selected jumps across material boundaries (discontinuous gradient or value)

- **Conformal Decomposition Finite Element Method (CDFEM)**
  - Enrichment by adding nodes along interfaces

CDFEM Uses Ideas From XFEM, Level Set Methods, and ALE Moving Mesh

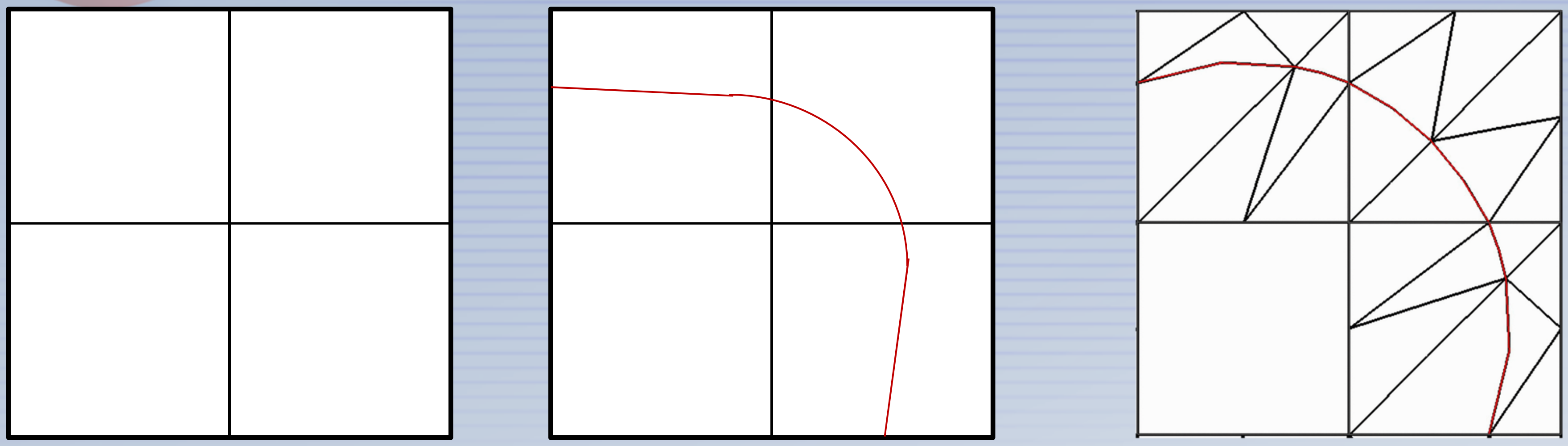

Base mesh

Level Set Function

CDFEM Mesh added dynamically at interface

Benefits: Meshed free surface allows for easy application of boundary conditions, discontinuous variables are straight forward, topological changes

Drawbacks: Mass loss similar to diffuse interface methods, expensive, file bloat

- CDFEM shown convergent for steady flow, Noble et al, IJNMF, 2010
- Extension to moving boundary problems

Moving CDFEM

- How do we handle the moving interface?
- What do we do when nodes change sign?
- What space do we use for pressure, velocity and level set?

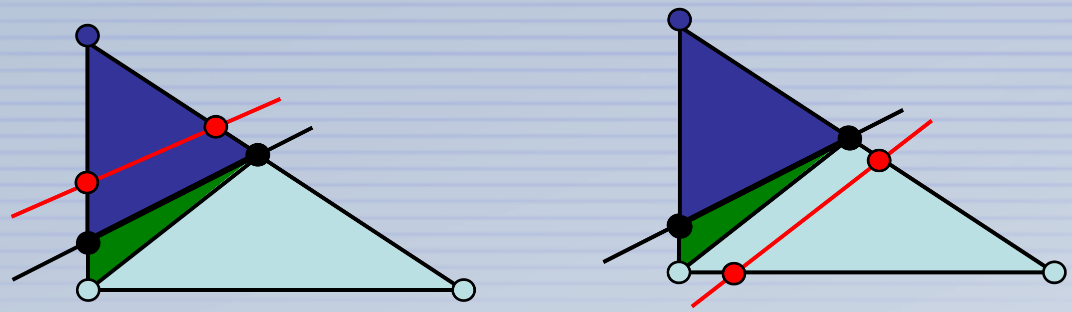

- Goals
  - Try to recover moving mesh case for moving interface
  - Try to preserve minima, maxima
  - Smooth interface
- Proposal
  - Prolongation: Set “old” value to value of nearest point on interface
  - Dynamics: Use ALE style (u-dxdt) for advection term
  - Allow velocity gradient and pressure jumps across interface
  - Level set on sub-element mesh

CDFEM – Unconstrained Spaces for Stability and Robustness

Discrete Space Considerations in CDFEM

- Anecdotal evidence for space requirements
  - Static, diffusive problems have shown optimal convergence rates using subelements
  - Dynamic, advection problems have shown poorly controlled modes in pressure-velocity and level set fields
- New formulation shows stable behavior for all fields on cut mesh
- This allows for jumps in pressure across interfaces due to capillarity since two pressure fields are used
- Level set and velocity are continuous across interface, but gradients can be discontinuous
- This allows for jumps in velocity gradient across interfaces
- Finite element formulation is PSPG stabilized on piecewise linear triangles (2D) or tetrahedrals (3D)
- Surface stabilization term included for problems with surface tension (Hysing …)

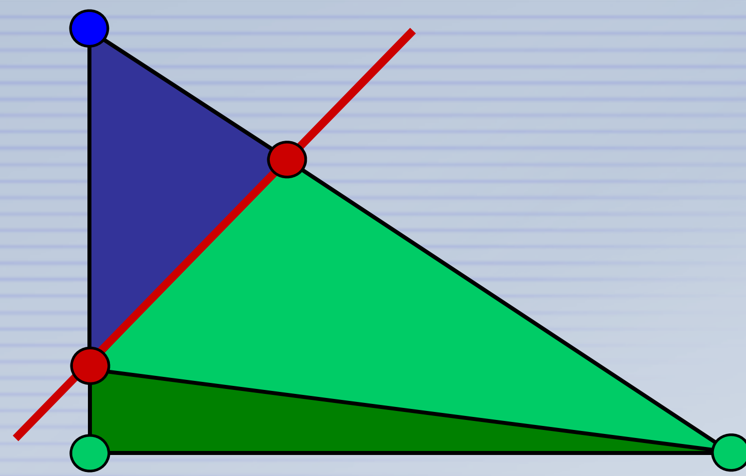

Discrete spaces used in this work

- Level set is PL on cut element
- Velocity is PL on cut element allowing gradient jump across interface
- Pressure is PL on cut element for each phase (separate PL field for each phase)

Formulation: Capillary Hydrodynamics

Navier - Stokes

- Incompressible, Newtonian

$$\nabla \cdot u = 0,\ \rho \frac{\partial u}{\partial t} + \rho u \cdot \nabla u = -\nabla P + \nabla \cdot \mu\left(\nabla u + \nabla u^t\right) + \rho g$$

- Galerkin, Backward Euler, Moving mesh term

$$\int_\Omega \rho \frac{u - u^n}{\Delta t} N_i \, d\Omega + \int_\Omega \rho\left(u - \dot{x}\right) \cdot \nabla u \, N_i \, d\Omega +$$

$$\int_\Omega \left[-P\,I + \mu\left(\nabla u + \nabla u^t\right)\right] \cdot \nabla N_i \, d\Omega - \int_\Omega \rho g \, N_i \, d\Omega + \int_\Gamma S \, N_i \, d\Gamma = 0$$

- PSPG stabilization

$$\int_\Omega \nabla \cdot u \, N_i \, d\Omega + \int_\Omega \tau_u \left[-\nabla P + \rho g\right] \cdot \nabla N_i \, d\Omega = 0$$

- SUPG stabilization

$$N_i \Rightarrow N_i + \tau_u \, u \cdot \nabla N_i,\ \tau_u = \left[\left(\frac{2}{\Delta t}\right)^2 + u_i g_{ij} u_j + 12\left(\frac{\mu}{\rho}\right)^2 g_{ij} g_{ij}\right]^{-\frac{1}{2}}$$

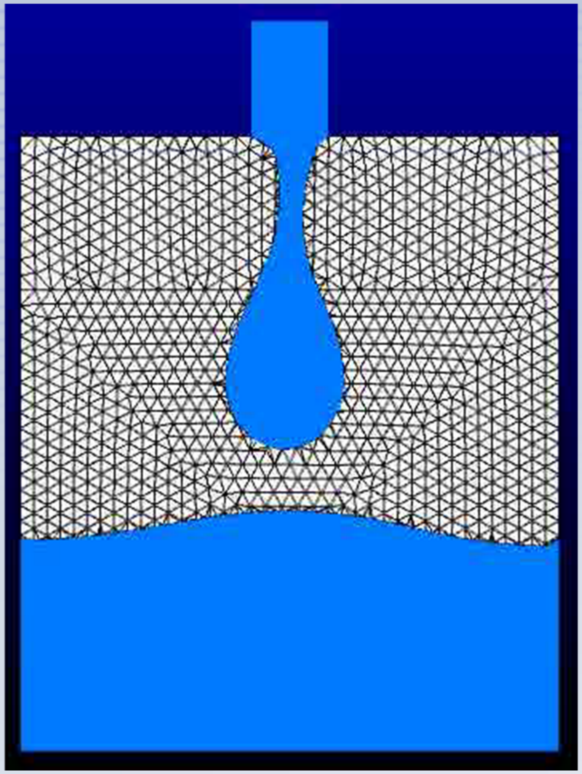

Formulation: Interface Dynamics

Level Set Equation

- Advection equation

$$\frac{\partial \phi}{\partial t} + u \cdot \nabla \phi = 0$$

- Galerkin, Backward Euler

$$\int_{\Omega} \frac{\phi - \phi^{n}}{\Delta t} N_i \, d\Omega + \int_{\Omega} u \cdot \nabla \phi \, N_i \, d\Omega = 0$$

- SUPG stabilization

$$N_i \Rightarrow N_i + \tau_{\phi} \, u \cdot \nabla N_i, \; \tau_{\phi} = \left[\left(\frac{2}{\Delta t} \right)^{2} + u_i g_{ij} u_j \right]^{-\frac{1}{2}}$$

- Periodic renormalization
  - Compute nearest distance to interface

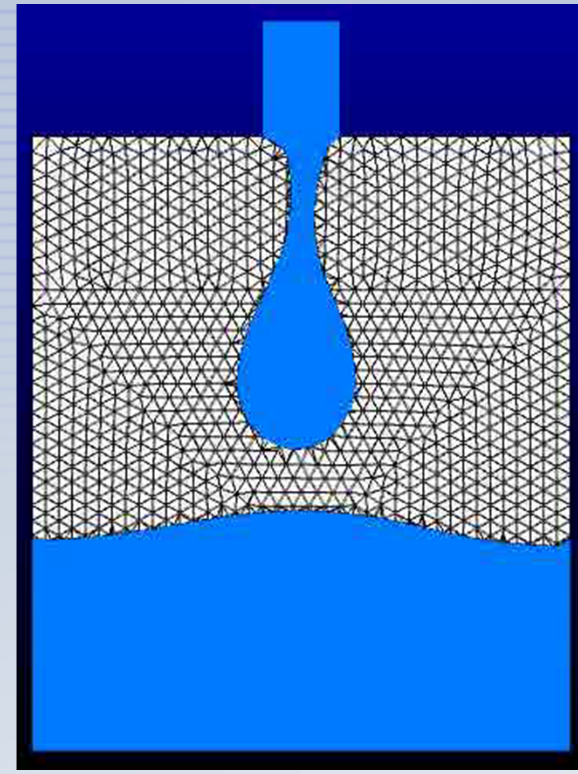

Models: Liquid-Air Interface

Capillary Force

- Same model used in ALE simulations
  - Jump in stress due to interfacial tension
  - Laplace-Beltrami implementation avoids second derivatives

$$\int_{\Gamma} \left(\gamma\kappa\,\mathbf{n} + \nabla_s \gamma\right) N_i \; d\Gamma = \int_{\Gamma} \gamma \nabla_s N_i \; d\Gamma,\ \nabla_s \equiv \left(\mathbf{I} - \mathbf{nn}\right)\nabla$$

Interface Stabilization

- Surface viscosity type stabilization
  - Based on recent paper by Hysing

$$\int_{\Gamma} \mu_s \nabla_s u \cdot \nabla N_i \; d\Gamma$$

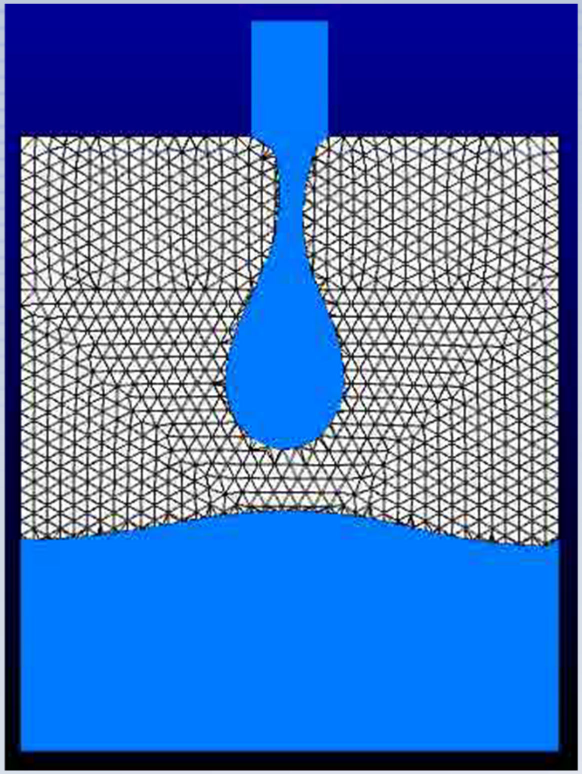

Code to Code Comparisons for 2D Buoyant Drop: Two Test Problems

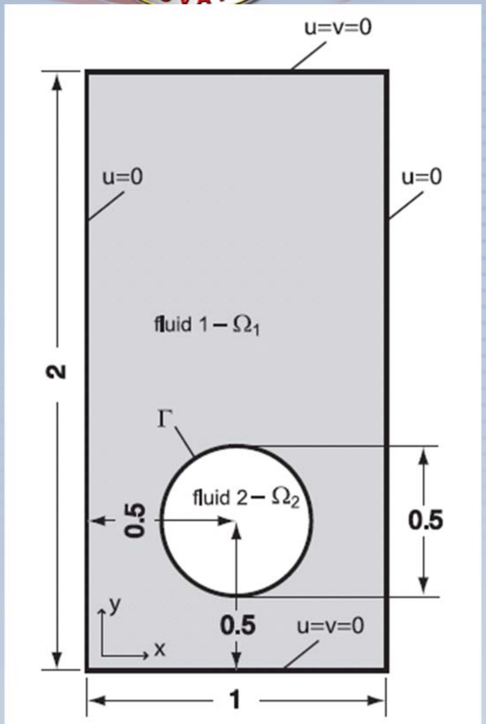

- Important dimensionless groups are the Reynolds number and the Eotvos number, and property ratios for the two fluids

$$\mathrm{Re} = \frac{2\rho_1 U_g R_0}{\mu_1},\ Eo = \frac{2\rho_1 U_g^2 R_0}{\sigma},\ \frac{\rho_1}{\rho_2},\ \frac{\mu_1}{\mu_2}\ \text{where}\ U_g = \sqrt{2gR_0}$$

- Two test cases included
  - The first results in a smooth drop
  - The second has a fine trailing structure that must be captured

Table I. Physical parameters and dimensionless numbers defining the test cases.

Test case	ρ_1	ρ_2	μ_1	μ_2	g	σ	Re	Eo	ρ_1/ρ_2	μ_1/μ_2
1	1000	100	10	1	0.98	24.5	35	10	10	10
2	1000	1	10	0.1	0.98	1.96	35	125	1000	100

Hysing et al, “Quantitative benchmark computations of two-dimensional bubble dynamics, IJNMF, 2009

Code to Code Comparisons for 2D Buoyant Drop: Two Test Problems

Test 1

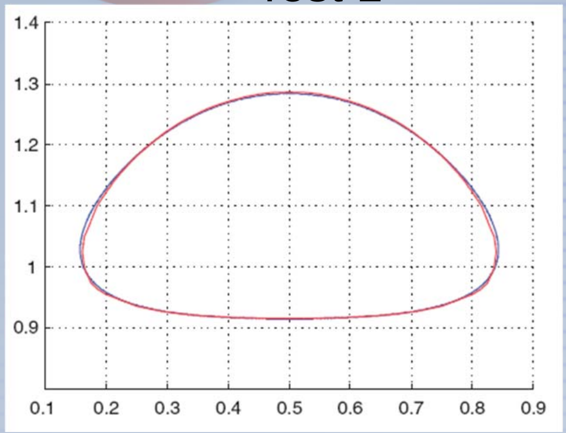

Diffuse level set

CDFEM

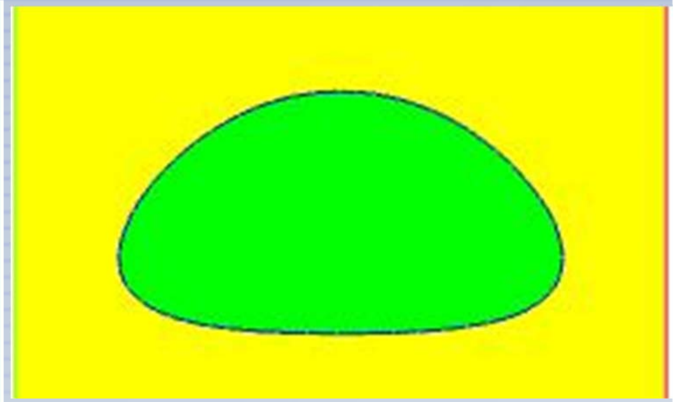

- Test 1 has gives a smooth drop shape
- Density and viscosity ratios of 10, Re=35 and Eo=10
- Both CDFEM and a classic diffuse interface method do a good job agreeing with each other and the benchmark
- Results given for coarse mesh (h=1/40)

Hysing et al, "Quantitative benchmark computations of two-dimensional bubble dynamics, IJNMF, 2009

Code to Code Comparisons for 2D Buoyant Drop: Two Test Problems

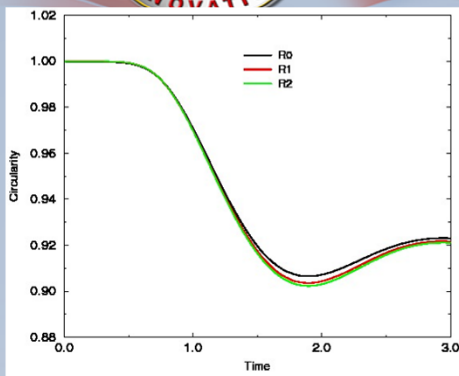

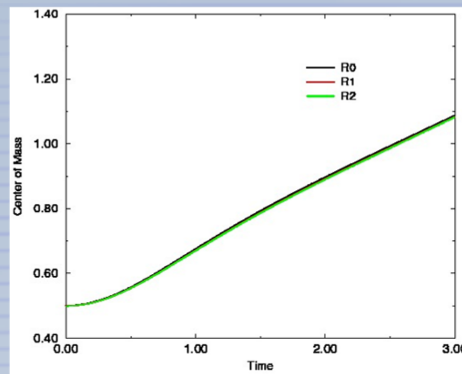

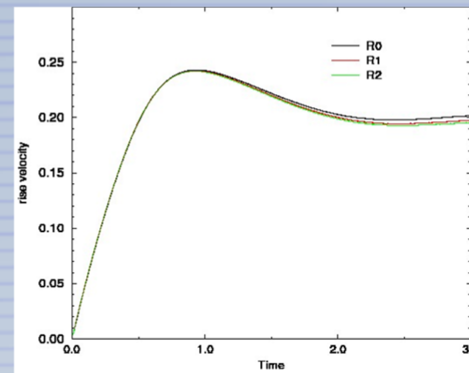

CDFEM
Test 1

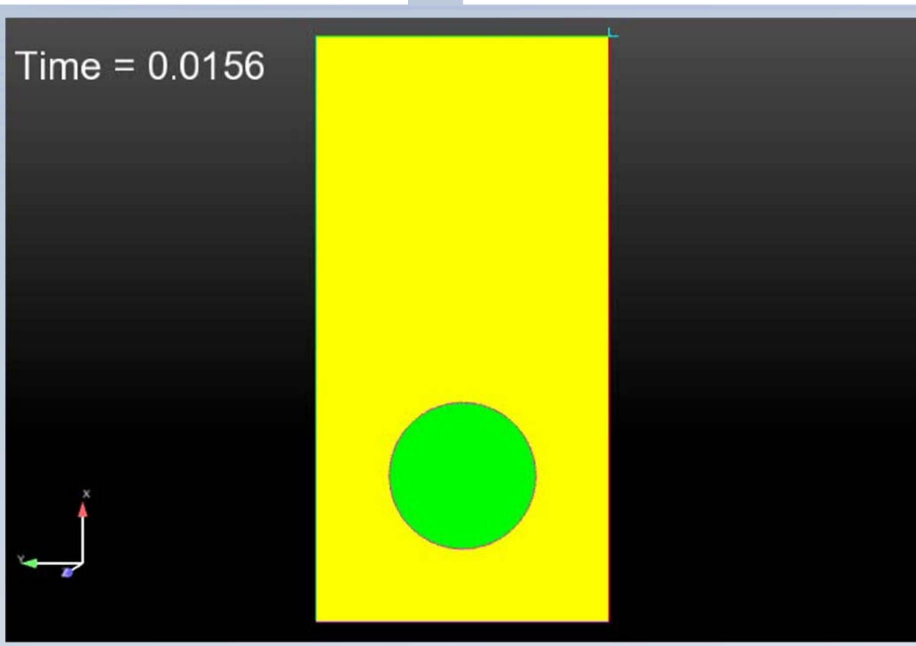

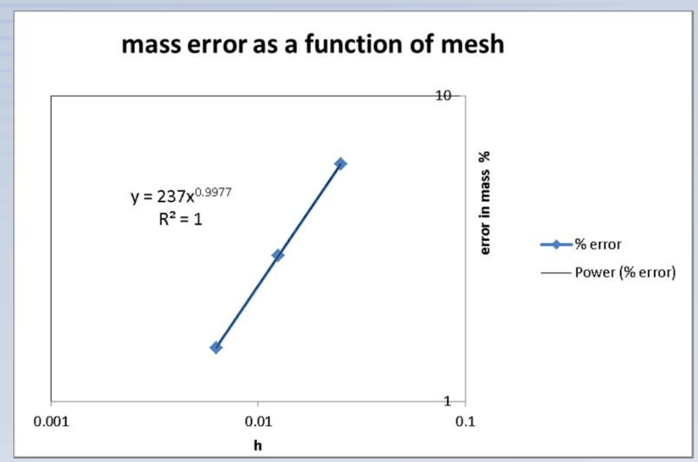

Test 1 shows good convergence with mesh refinement for center of mass, circularity and rise velocity metrics

Hysing et al, “Quantitative benchmark computations of two-dimensional bubble dynamics, IJNMF, 2009

Code to Code Comparisons for 2D Buoyant Drop: Two Test Problems

Diffuse level set

CDFEM

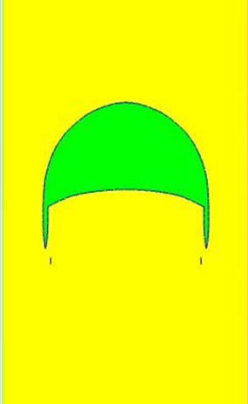

- Test 2 has fine trailing structures that must be captured by the code
- Density ratio of 1000 and viscosity ratios of 100, Re=35 and Eo=125
- Both CDFEM and a classic diffuse interface method do a reasonable job, but give disparate results
- Results given for coarse mesh (h=1/40)

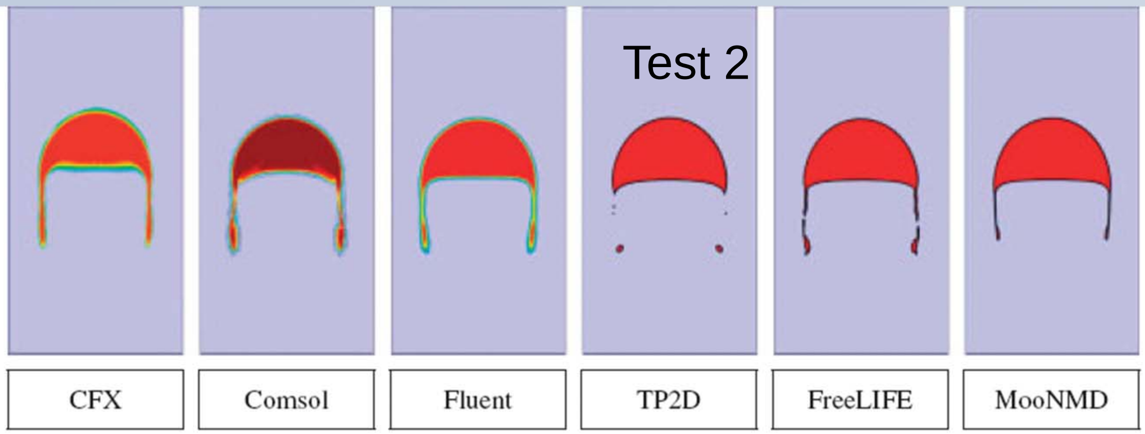

Figure 1. Numerical simulations of a two-dimensional rising bubble for six different codes with identical problem formulations.

Hysing et al, “Quantitative benchmark computations of two-dimensional bubble dynamics, IJNMF, 2009

Mesh refinement study: Constrained CDFEM

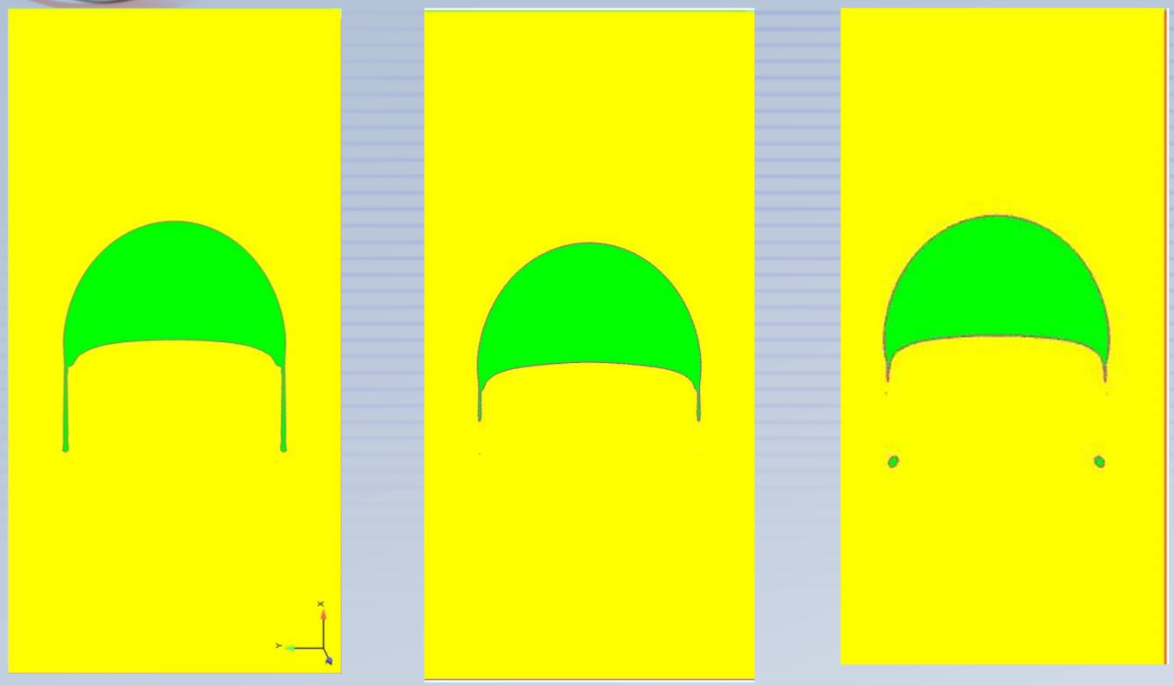

h=1/40 h=1/80 h=1/160

Δt=h/16

CDFEM with constrained pressure, velocity and level set

Constrained Velocity for Both Phases on h=1/40 Mesh

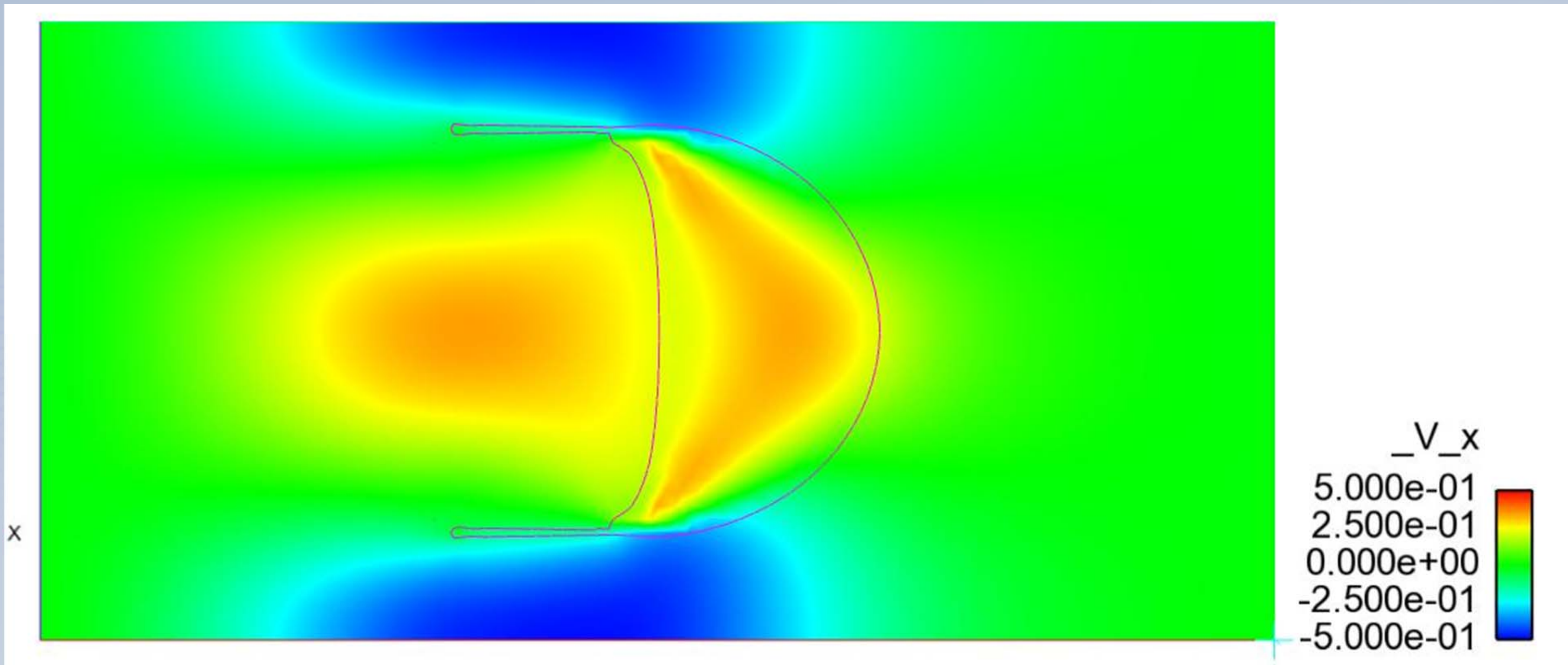

- Constraining velocity to be continuous across the interface creates a stable algorithm
- Smoothed jump in velocity occurs one row of elements in from the interface

Mesh Refinement Study: Rise Velocity

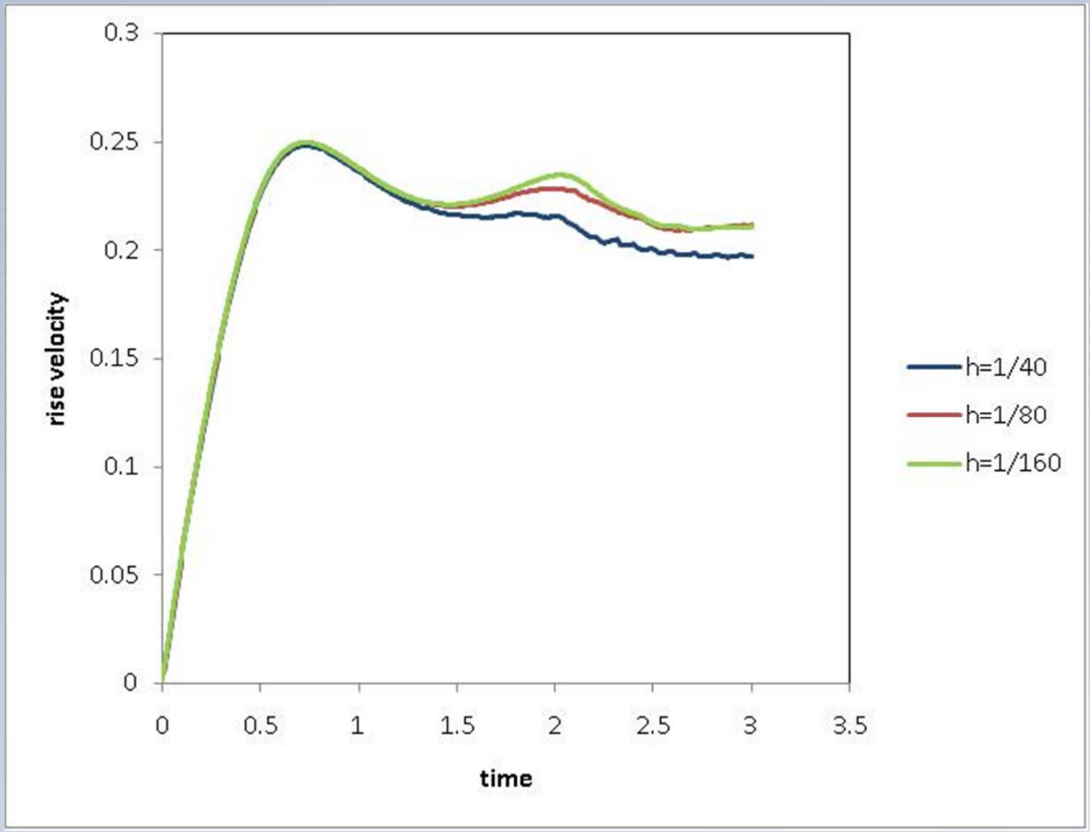

Rise velocity is defined as velocity in gravity direction over the area of the bubble

$$\text{rise velocity} = \frac{\int_A u_x \, dxdy}{\int_A 1 \, dxdy}$$

Comparison to Hysing et al, 2009

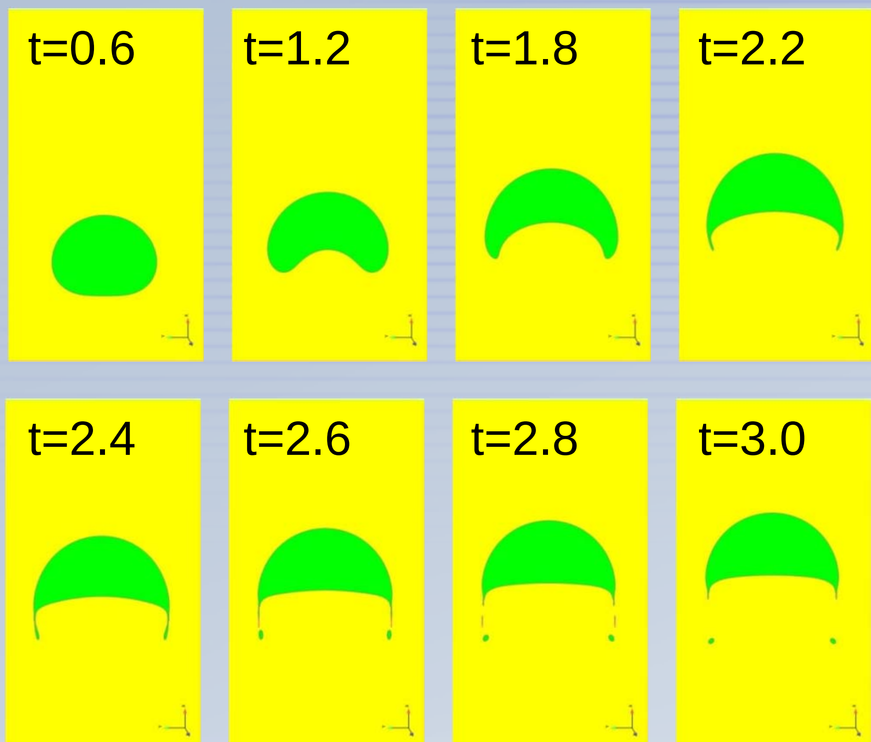

CDFEM with constrained pressure, velocity, and level set, h=1/160

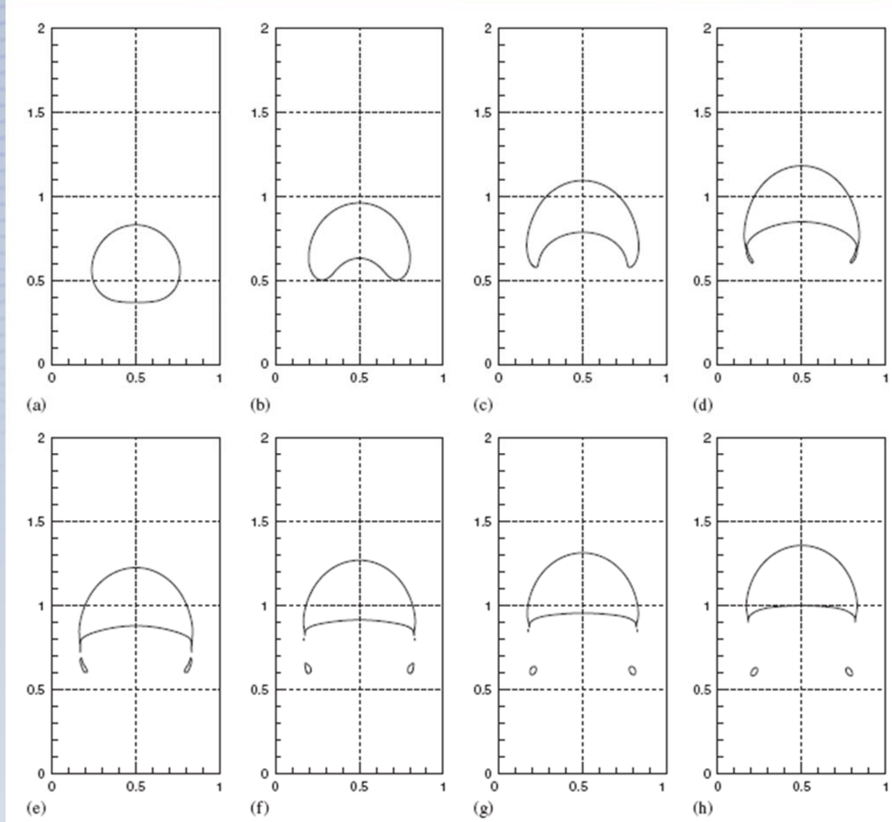

Figure 15. Typical time evolution of the interface for test case 2: (a) $t=0.6$; (b) $t=1.2$; (c) $t=1.8$; (d) $t=2.2$; (e) $t=2.4$; (f) $t=2.6$; (g) $t=2.8$; and (h) $t=3.0$.

2D Rayleigh-Taylor Instability

- Unstable stratification of heavy fluid over light fluid
- Problem similar to Rayleigh-Taylor instability from Smolianski (IJNMF, 2005) but with a 2:1 aspect ratio instead of a 4:1
- Initial condition for the shape of the interface affects wave number and symmetry of instability
- Results for zero surface tension with fine mesh: h=1/80, dt=h/3

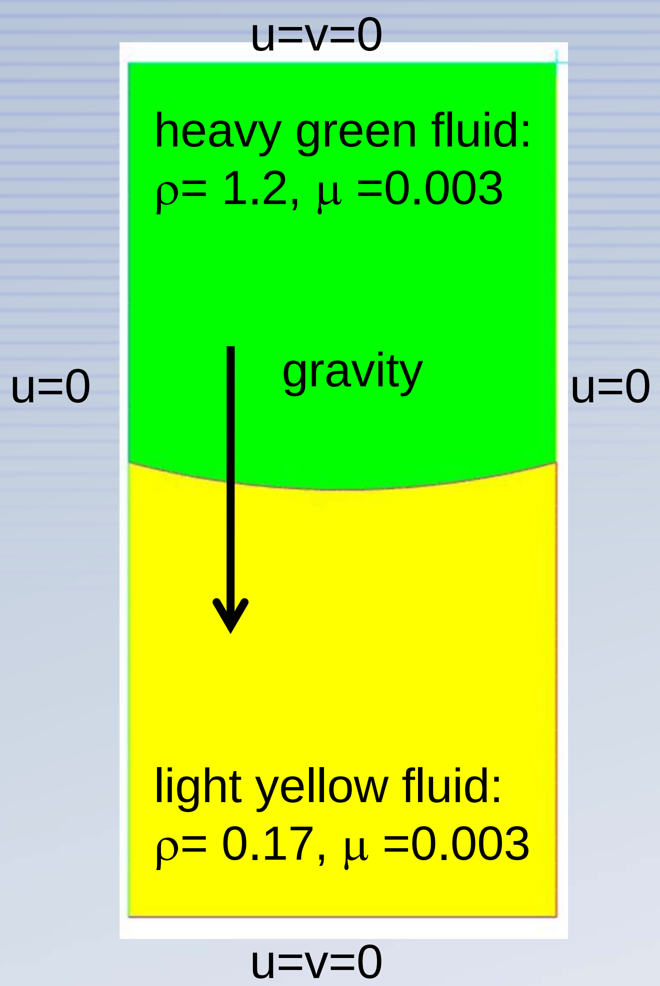

Rayleigh-Taylor instability with no surface tension
Unconstrained CDFEM, 1 pressure

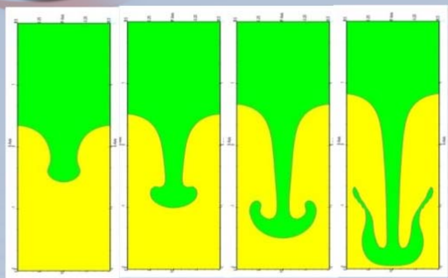

2.254% (1.95493)
h=1/20; Δt=h/3

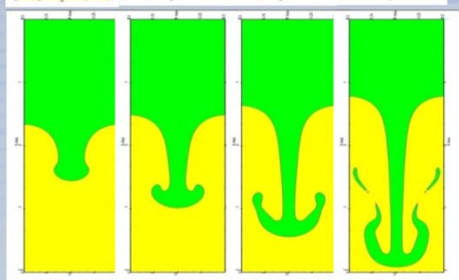

1.014% (1.97972)
h=1/40; Δt=h/3.0

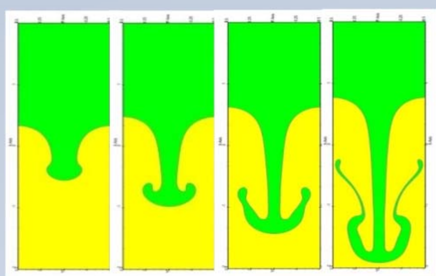

0.89% (1.9822)
h=1/80; Δt=h/3.0

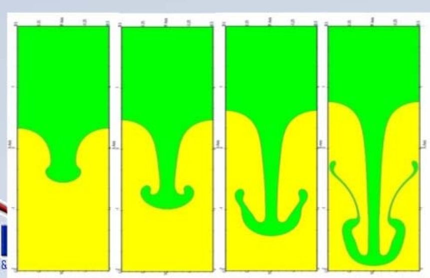

0.145% (1.9971)
h=1/160; Δt=h/3.0

- Metric is maximum area loss in the first 4s (t=1.96, 2.6, 3.3, 4.0)
- Initial area is 2.0
- Convergence looks is higher than first order (constrained is lower)
- Filament breakage/topology change may be the issue
- Renormalize every 0.05s

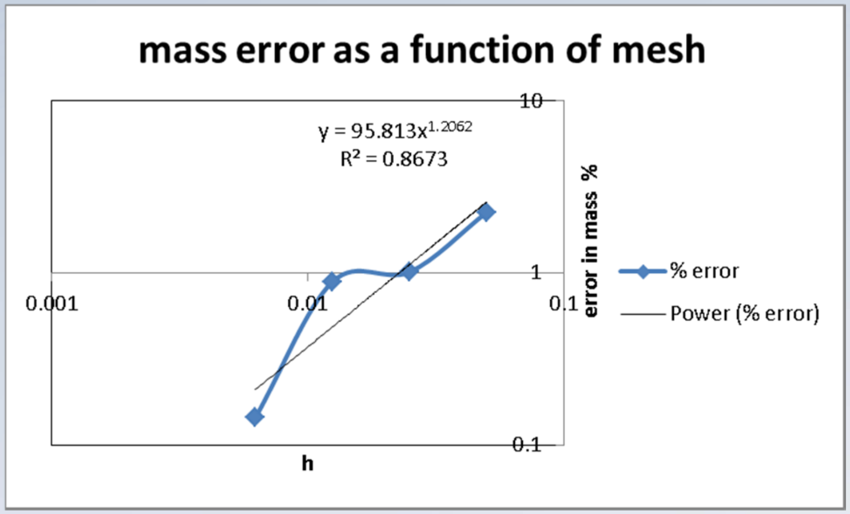

Droplet-scale Experiment in Microfluidic Device

- Create uniformly sized droplets
  - *Flow Focusing Microchannel*
- Understand flow field inside/around droplets
  - *Phantom high speed camera*
- Understand liquid-liquid mass transfer
  - *Ocean Optics spectrophotometer*

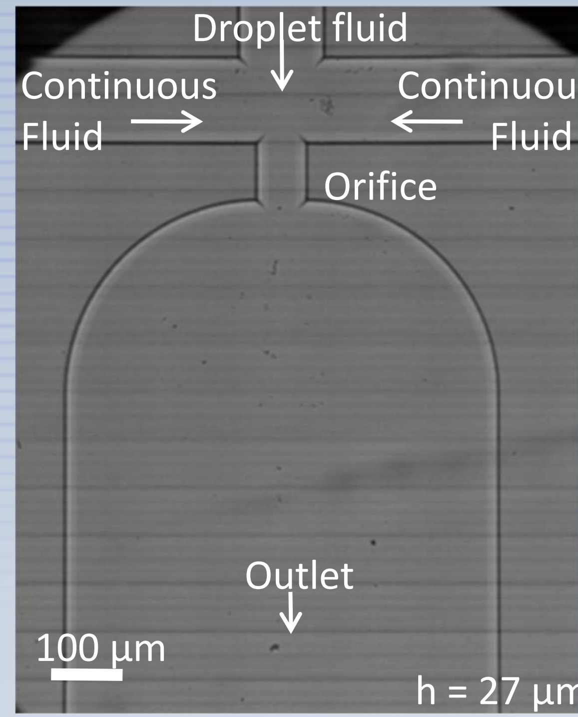

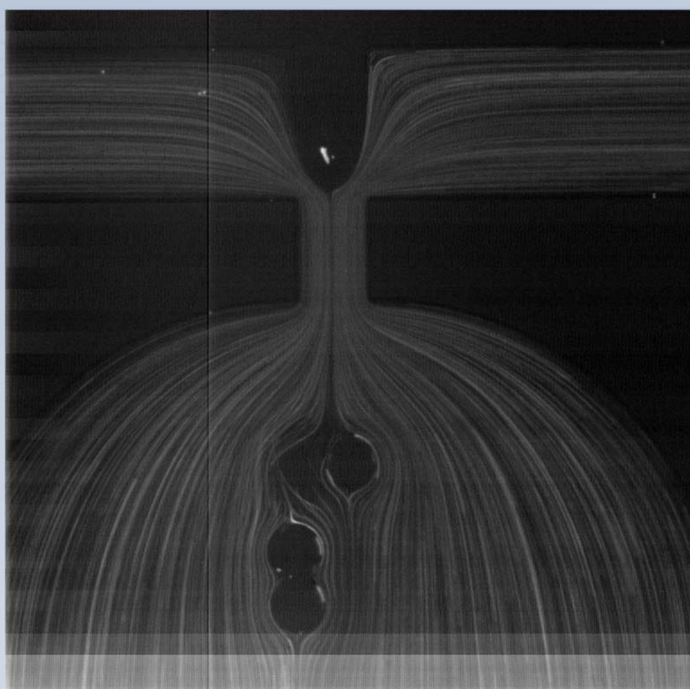

Decreasing inner flow rate

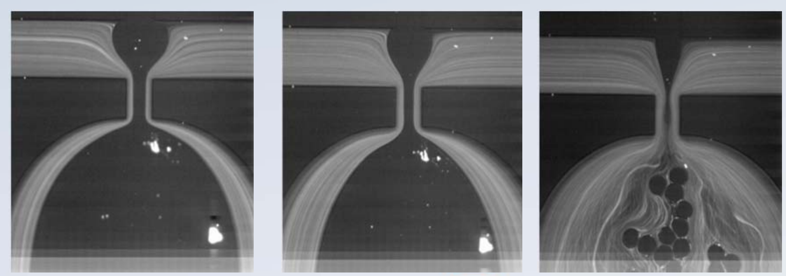

LDRD
LABORATORY DIRECTED RESEARCH & DEVELOPMENT

Sandia National Laboratories

Droplet Generator

Comparison with Experiment*

Droplet Fluid:
- Dodecane
- 0.74 g/cm^3
- 1.8 cSt
- 0.01 ml/hr

Continuous Fluid:
- Water
- 1.0 g/cm^3
- 1.0 cSt
- 0.5 ml/hr

Surface Tension:
- 52 mN/m

Dimensions:
- $2a$ = 200 microns
- W_c = 200 microns
- L_{or} = 110 microns
- W_{or} = 120 microns
- W_{out} = 500 microns

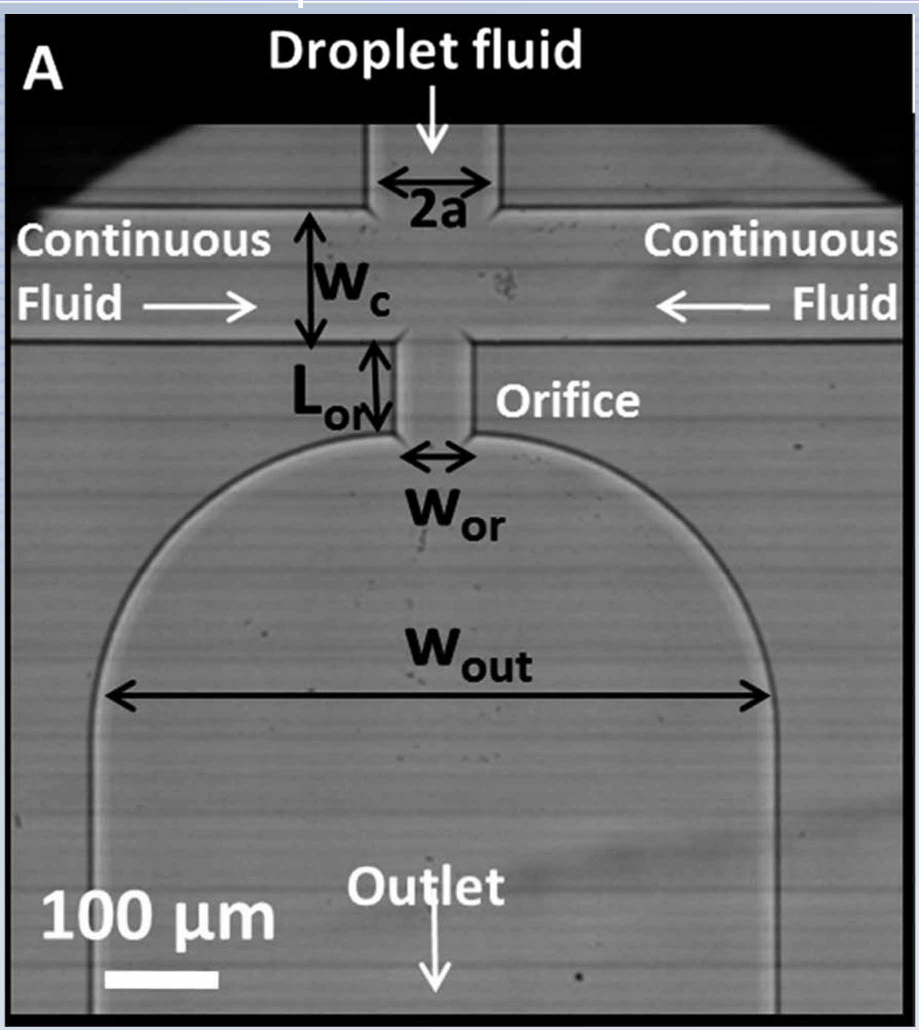

*Roberts, CC. et al. Comparison of monodisperse droplet generation in flow-focusing devices with hydrophilic and hydrophobic surfaces, Lab Chip, 2012, 12, 1540.

Droplet Generator (2D)
Comparison with Experiment

Experiment

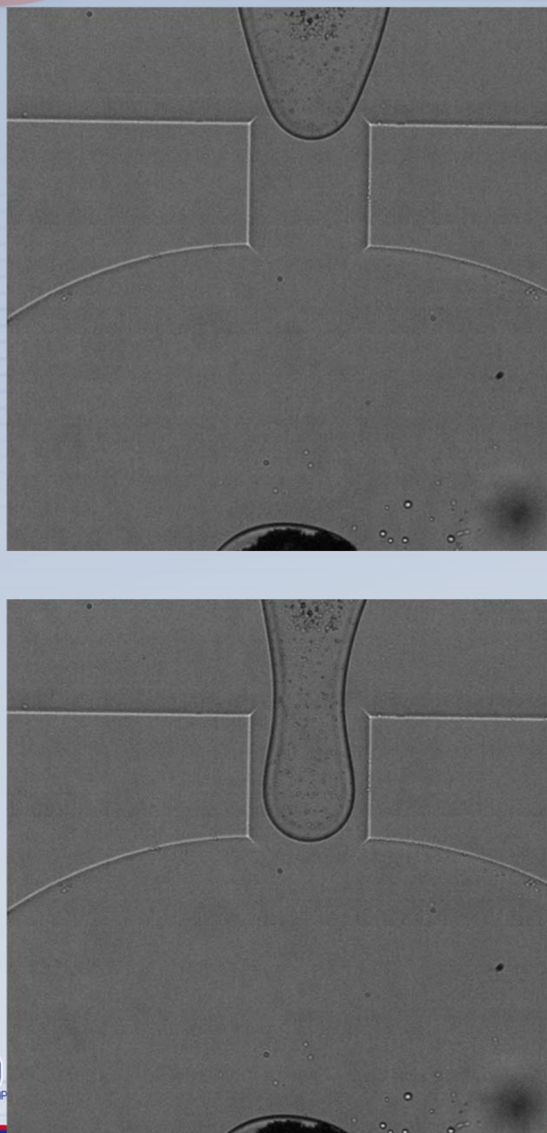

2D CDFEM

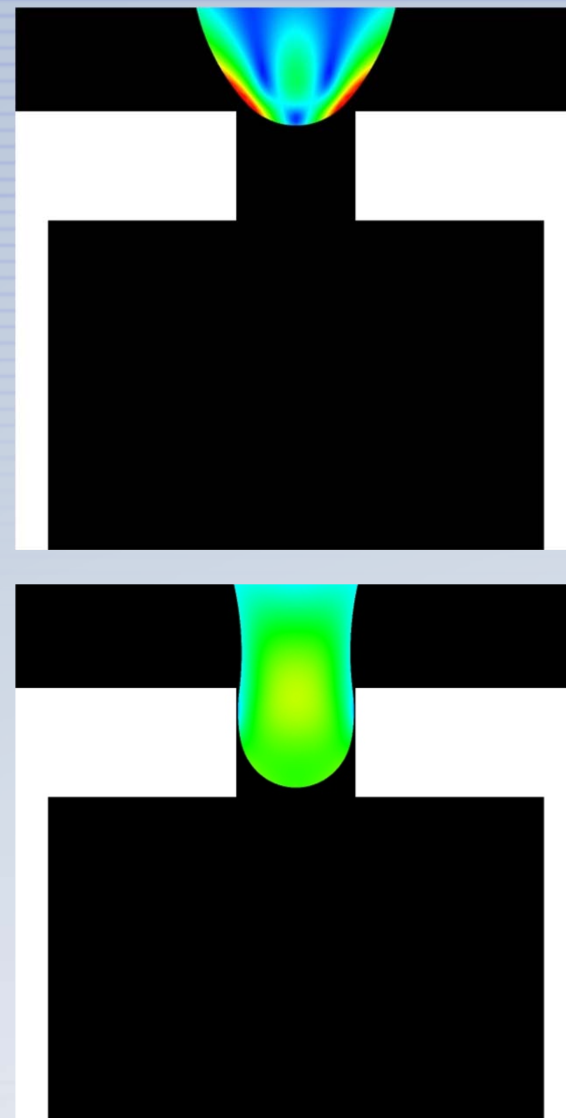

Droplet Generator (2D)

Comparison with Experiment

Experiment

2D CDFEM

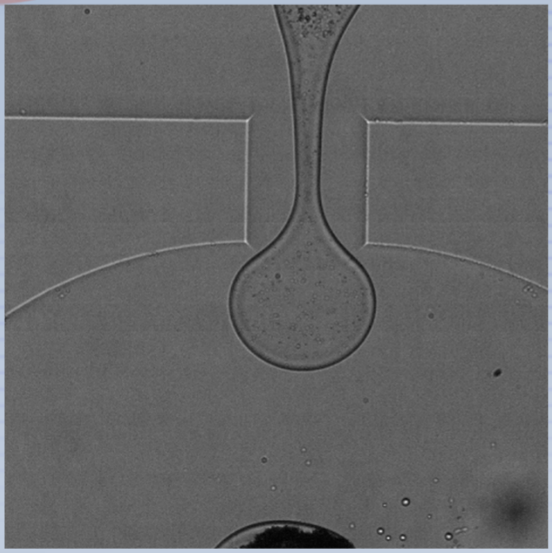

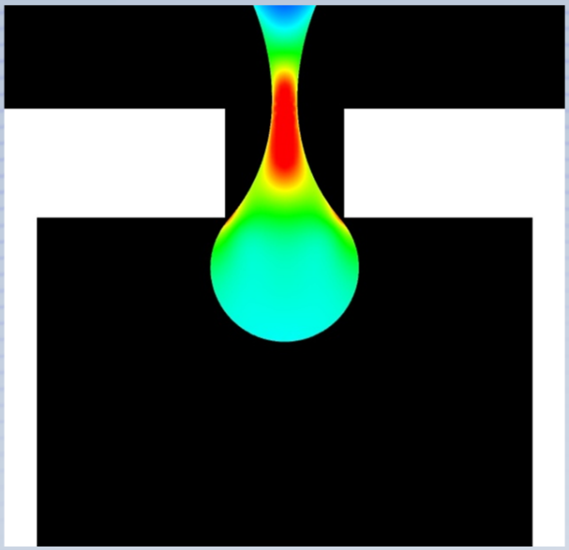

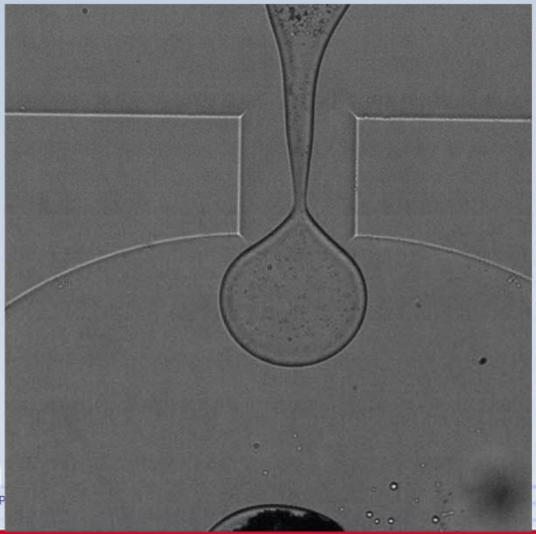

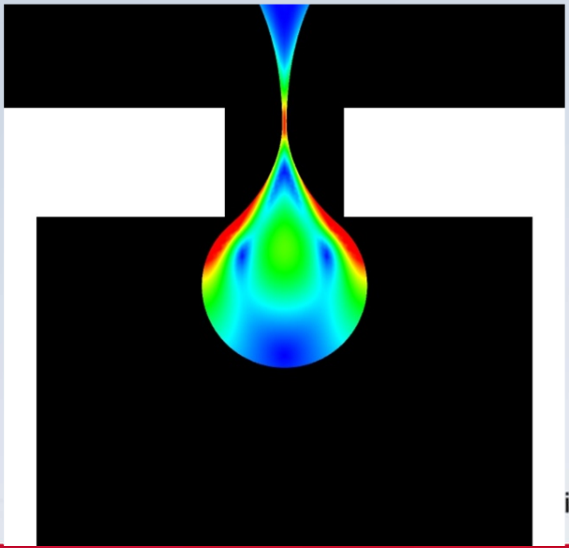

Droplet Generator (2D)

Droplet Formation

Droplet Fluid:
- Dodecane
- 0.74 g/cm^3
- 1.8 cSt
- 0.01 ml/hr

Continuous Fluid:
- Water
- 1.0 g/cm^3
- 1.0 cSt
- 0.5 ml/hr

Surface Tension:
- 52 mN/m

Dimensions:
- $2a$ = 200 microns
- W_c = 200 microns
- L_{or} = 110 microns
- W_{or} = 120 microns
- W_{out} = 500 microns

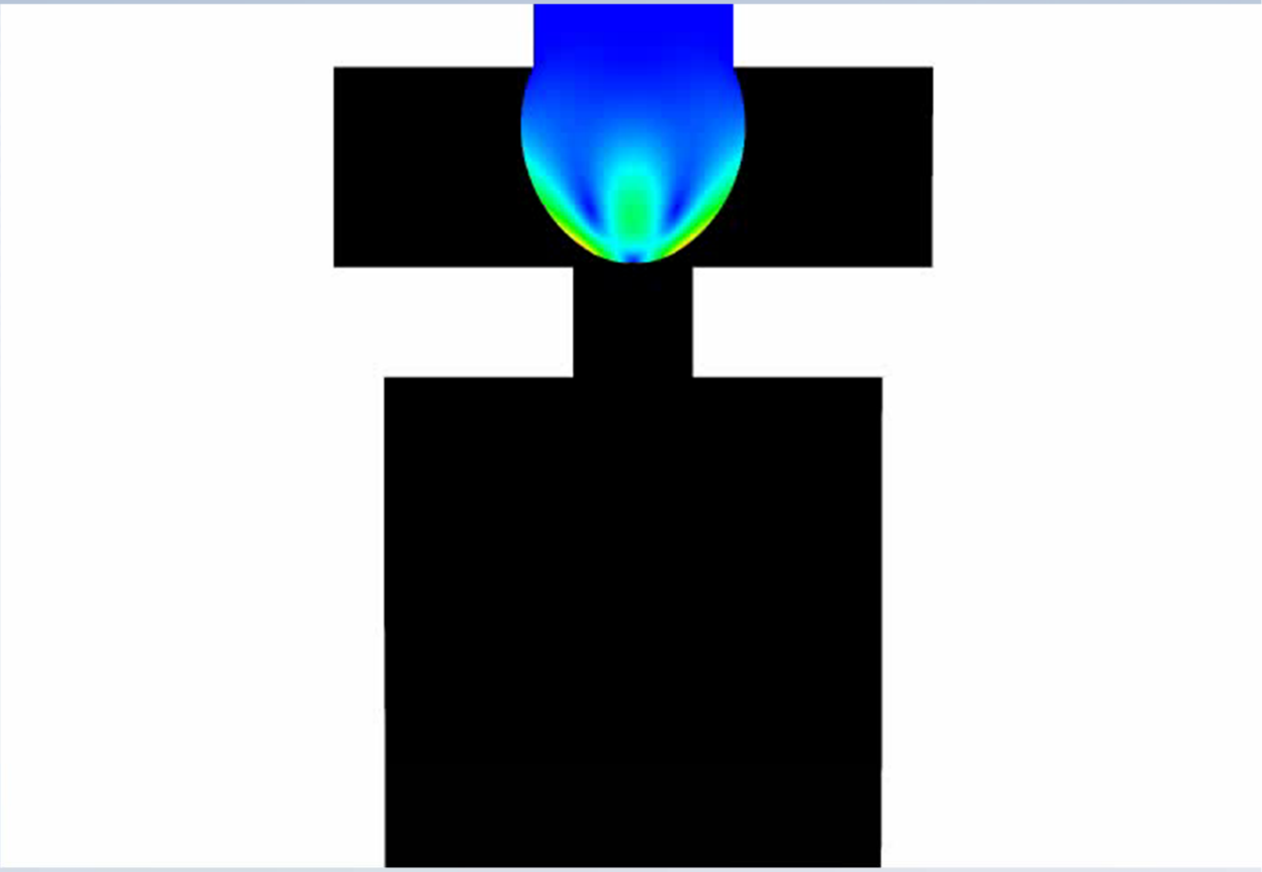

Droplet Generator (2D)

Velocity Magnitude

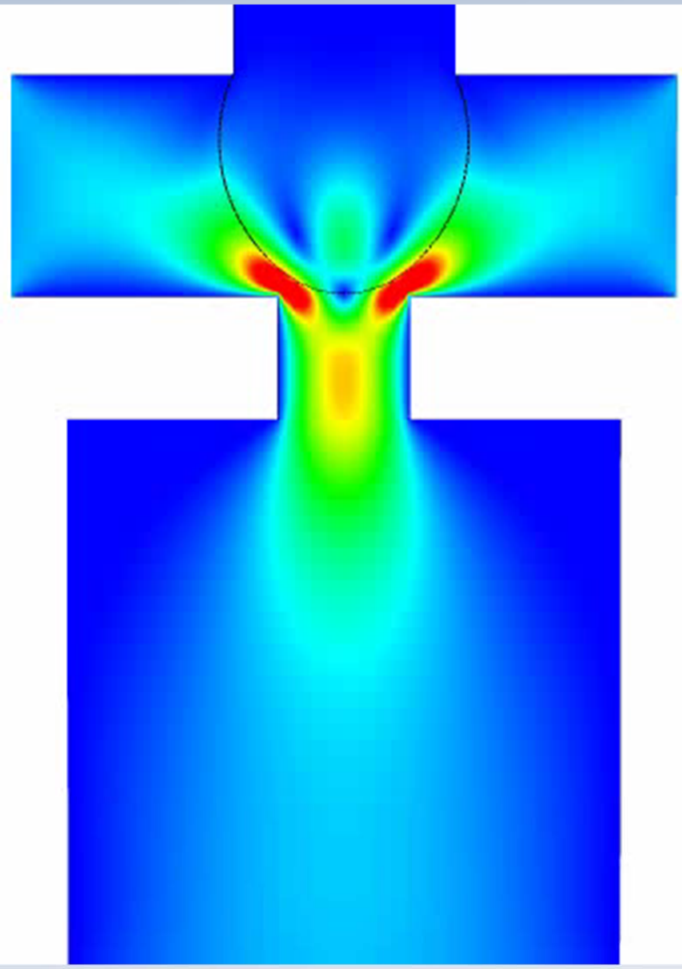

Droplet Generator (3D)

Droplet Formation

h = 27 microns

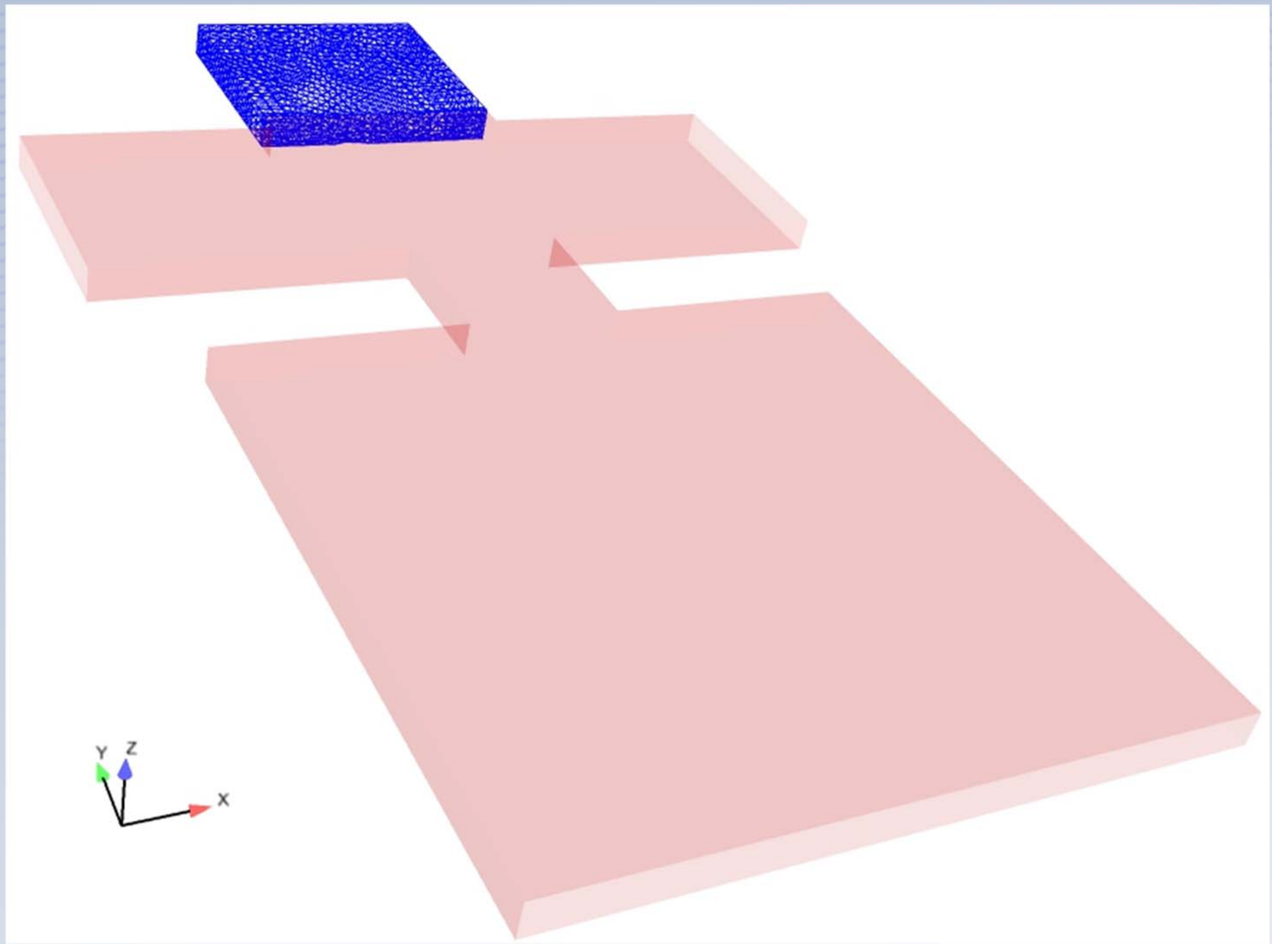

Droplet Generator (3D)

Droplet Formation

h = 27 microns

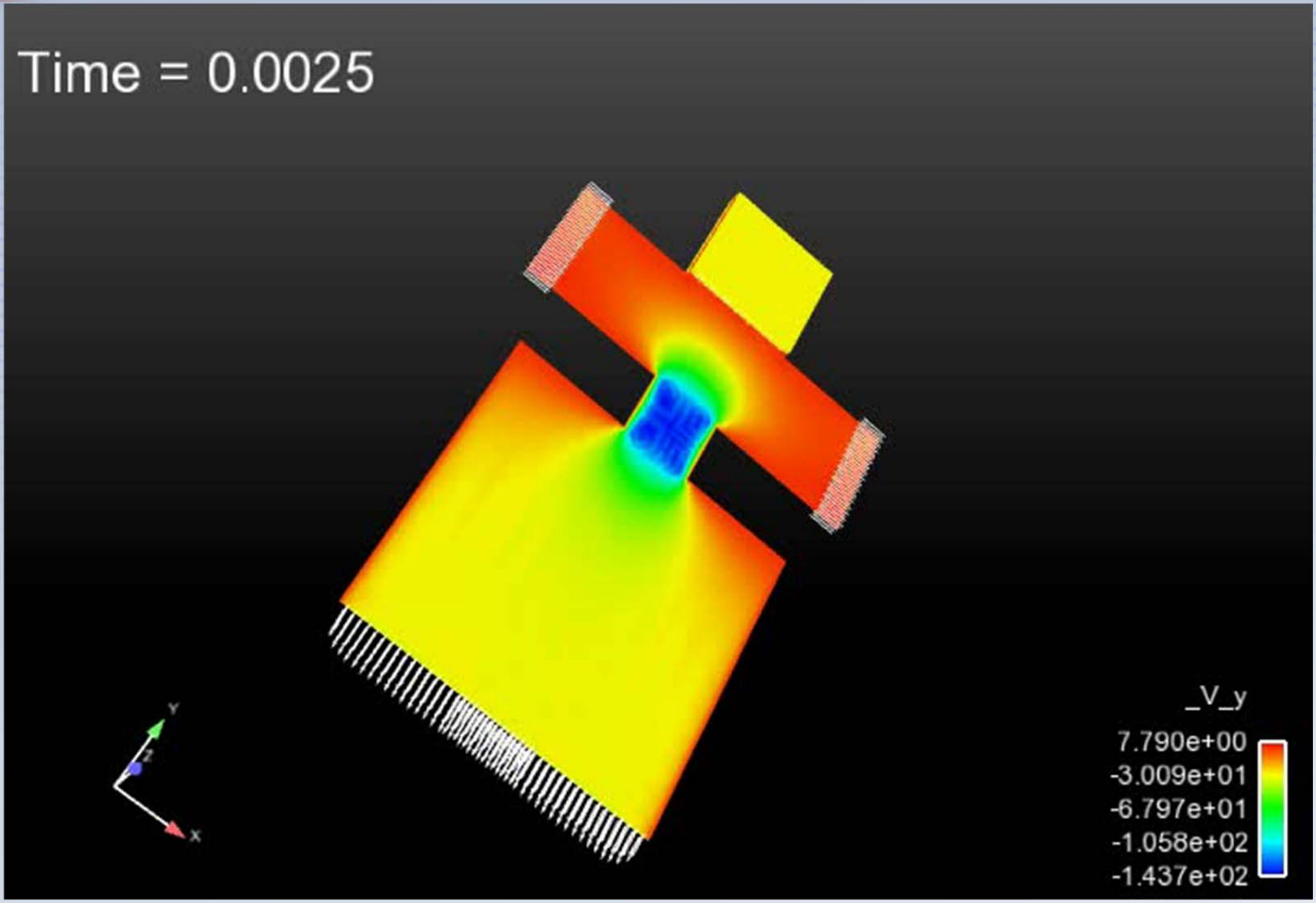

Mass Transfer Analysis Via Image Processing in Microfluidic Cell

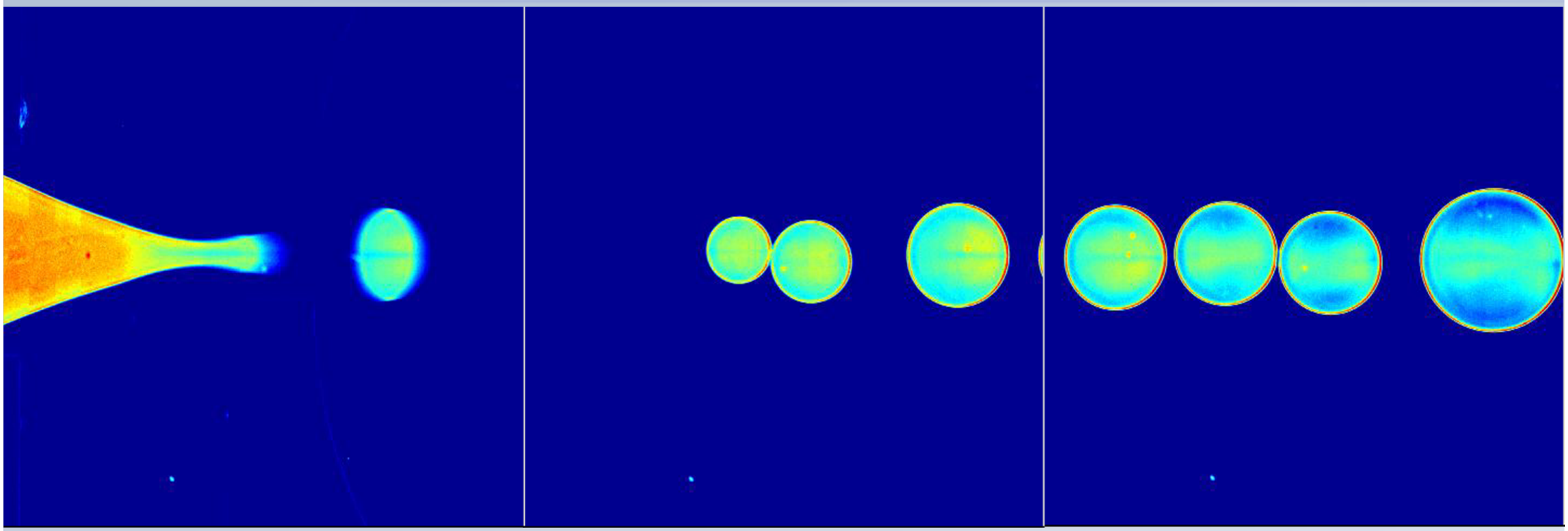

- Coalescence affects mass transport
- Internal flows remix coalesced drops
- Depletion occurs near boundaries

Drop D = 0.90 x Channel D

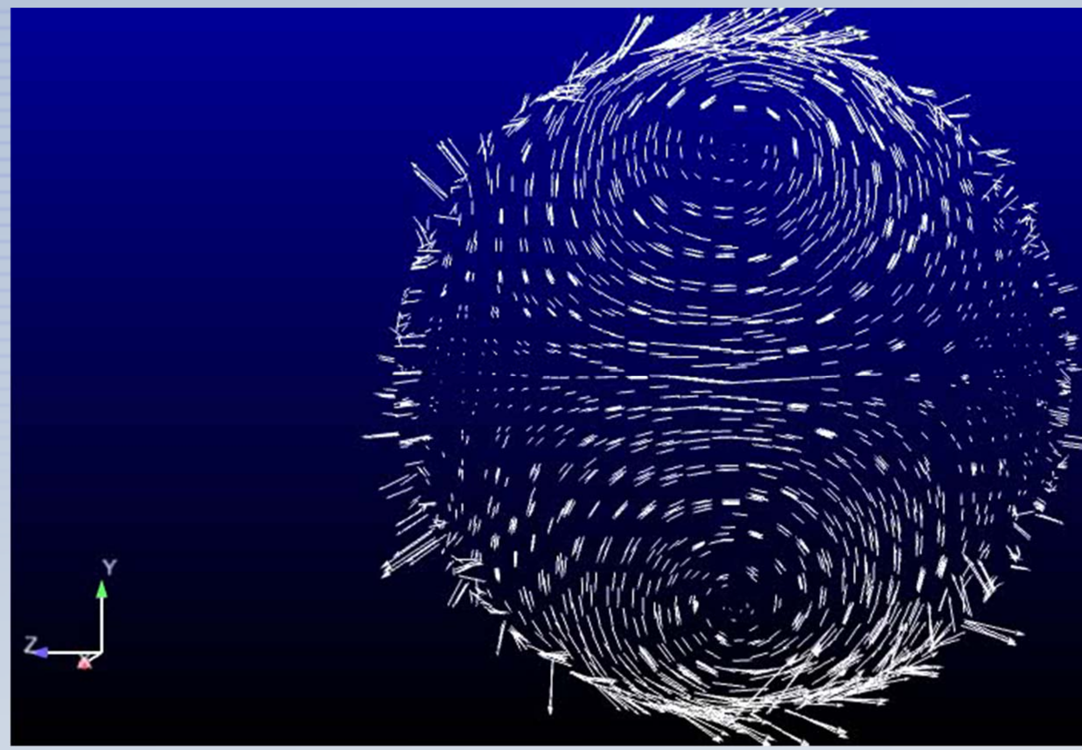

Experimental image looking at in plane velocities

CDFEM movie looking at in plane velocities

Squished drop

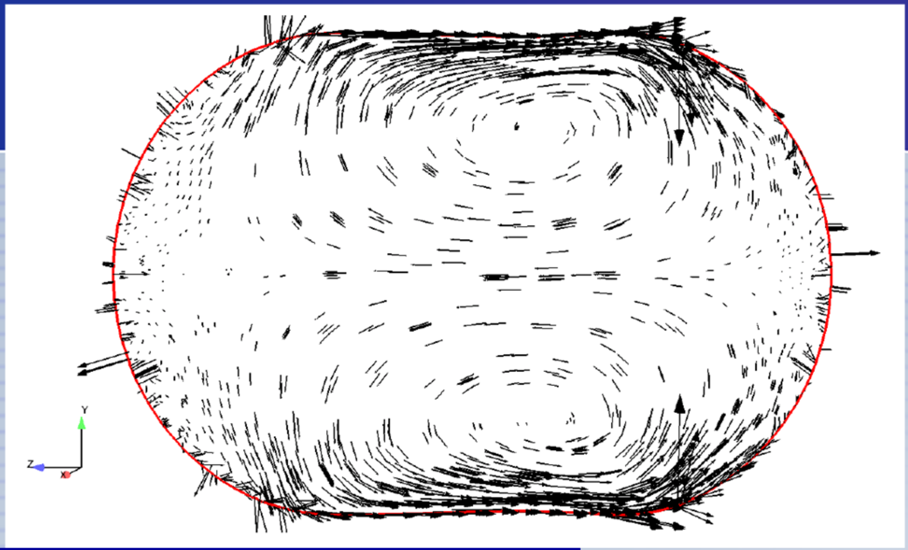

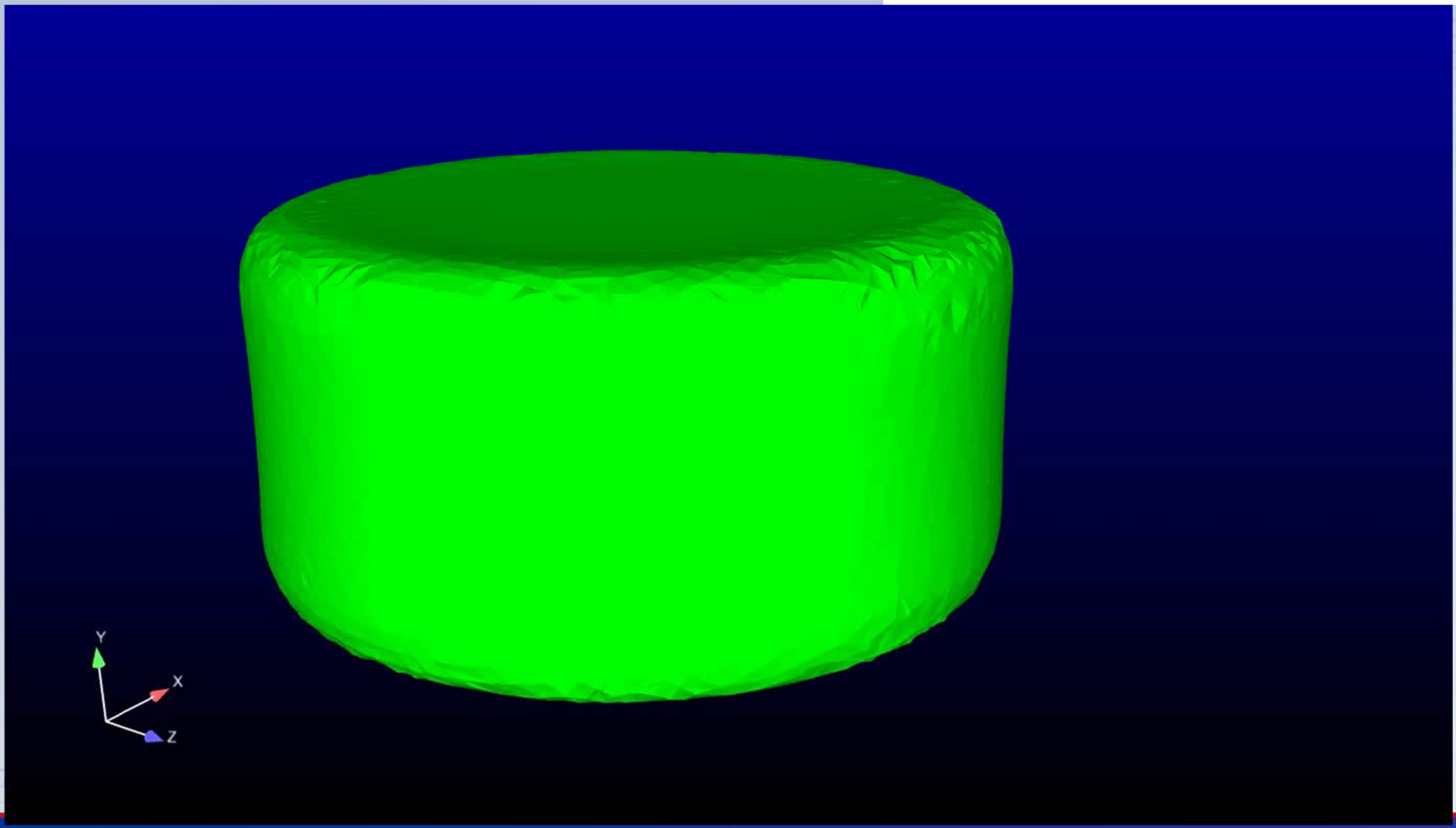

Sandia National Laboratories

Drop sliding down curved surface showing mesh refinement

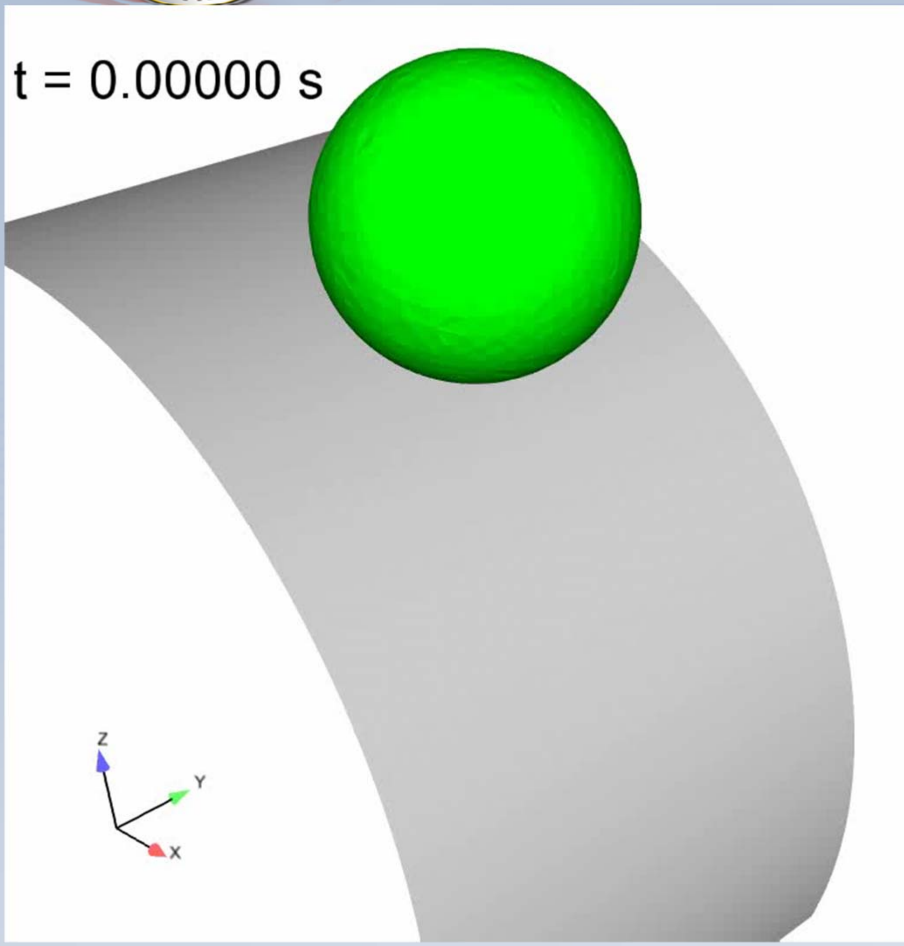

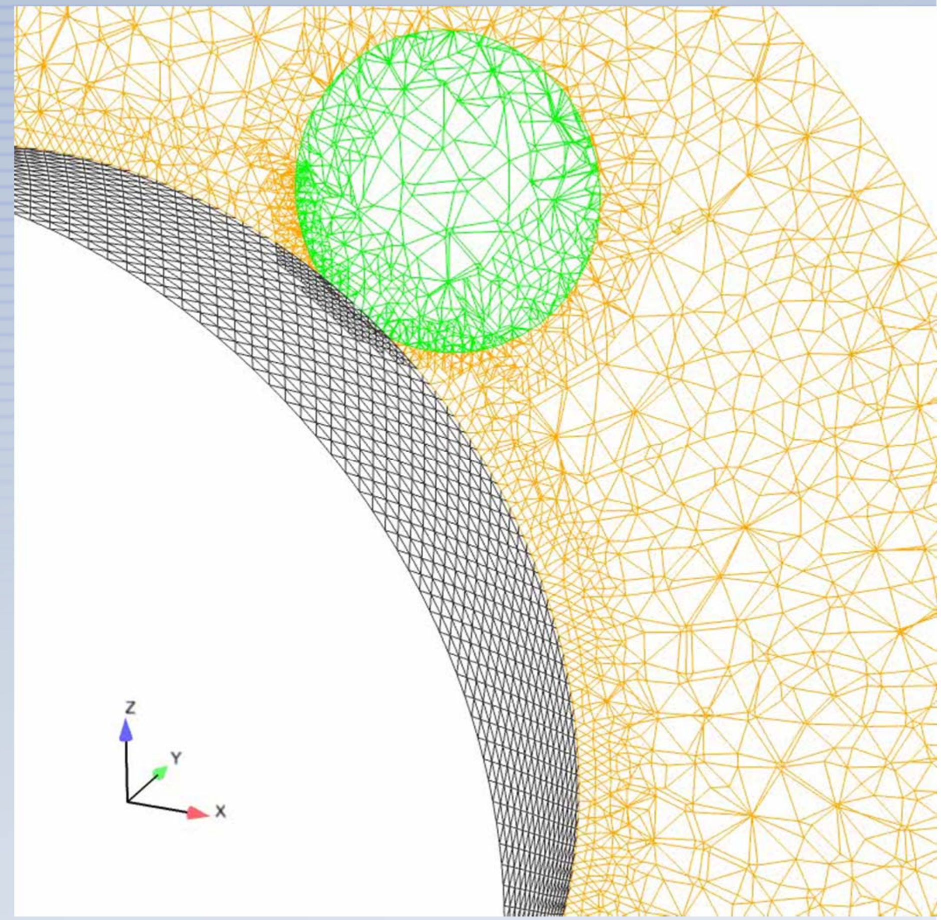

Conclusions and Future Work

- An unconstrained CDFEM algorithm has been developed and verified on a published 2D benchmark problem from Hysing et al, 2009

- CDFEM has been shown to be convergent with mesh refinement for smooth problems and for problems with topological changes

- Robustness in 3D still and issue with unconstrained formulation for low Ca

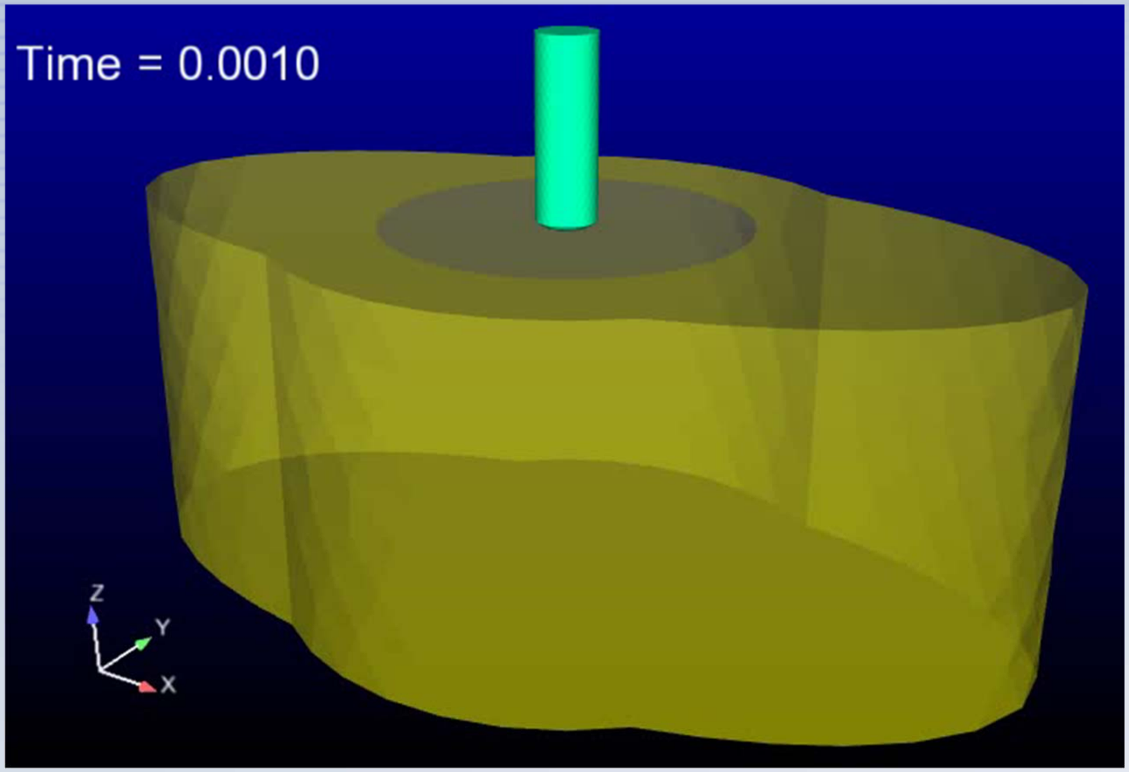

Working towards modeling mass transport with coalescence in a microfluidic device and eventually full contactor simulations

Coupling LAMMPS to CDFEM: Particulate Flow Applications

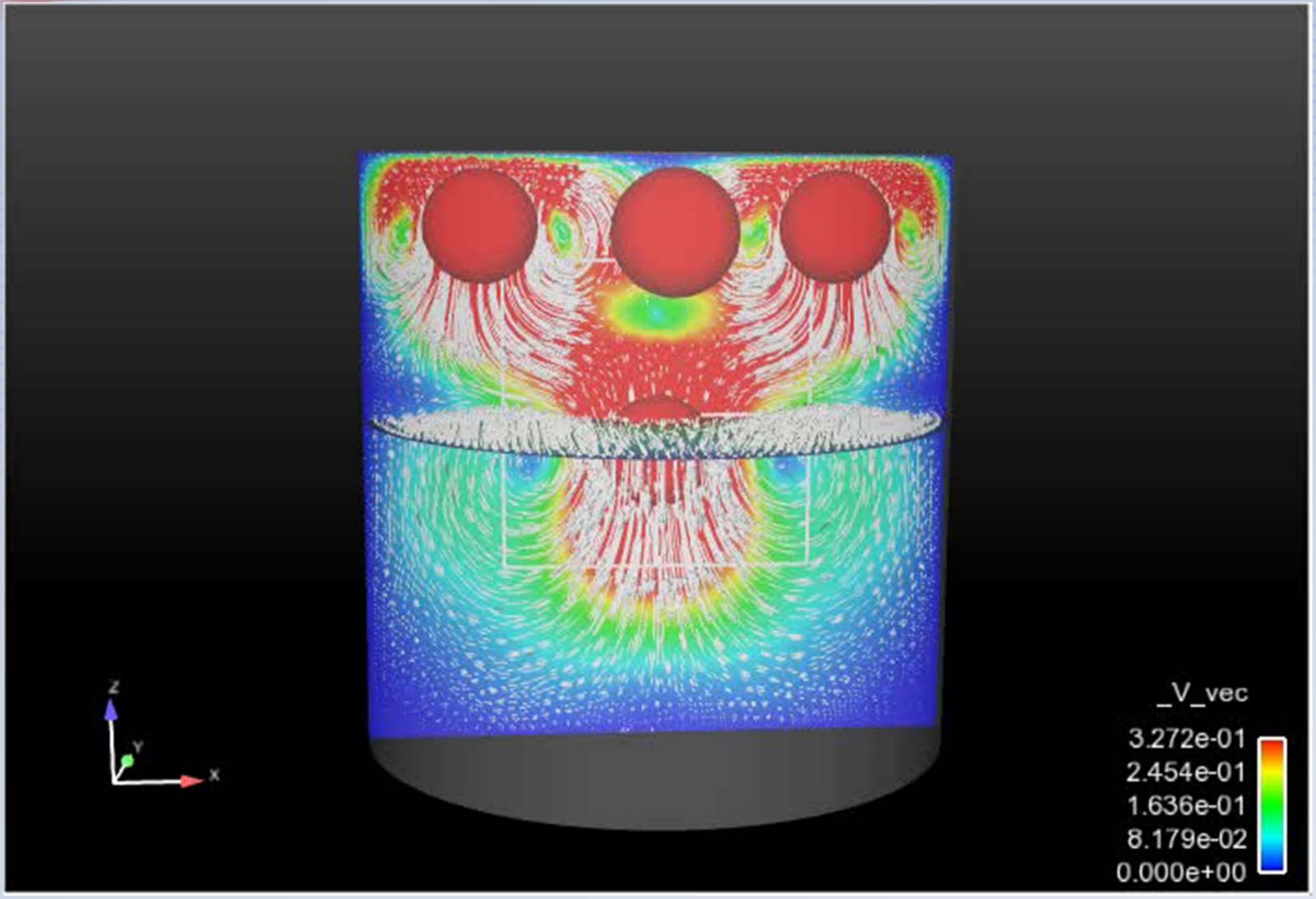

Jeremy Lechman, SNL